Critical Deposit Velocity in Slurry Flow

M. C. ROCO

Department of Mechanical Engineering
University of Kentucky
Lexington, KY 40506

C. A. SHOOK

Department of Chemical Engineering
University of Saskatchewan
Saskatoon, Canada S7N 0W0

INTRODUCTION

The critical deposit velocity in pipes and channels is often chosen as the lower limit at which slurry systems operate safely. In most cases, this limit exceeds the economic design velocity of single-phase (liquid) flow in pipes and strongly affects the efficiency of the slurry transport installations (Wiedenroth and Kirchner, 1972). For a given average concentration, the critical velocity depends on the distributions of the velocity and concentration in the whole flow cross section. Previous studies variously estimate the critical velocity in three ways:

1. From the dynamic equilibrium of solid particles at the bottom wall (Raudkivi, 1976; Hanks and Sloan 1981) (for low concentrations).
2. Using empirical correlations based on visual measurements or from capacitive or heated sensors (Durand, 1953; Ercolani et al., 1979).
3. Finding the velocity that minimizes the headlosses (Bain and Bonnington, 1970).

The effective flow structure is not determined in these approaches, and their areas of applicability are limited. The model recently developed for dense slurry flow (Roco and Shook, 1983a,b) enables us to compute the profile of the solids velocity at the pipe bottom. On this basis the critical velocity can be determined in a new way. In this paper we introduce a criterion for this threshold velocity using results for fine uniform sand slurry flows in pipes. Experimental distributions of the solid velocity and concentration measured in the laboratory were compared to the numerical predictions.

BASIC EQUATIONS

The suggested flow model is valid at low as well as high concentrations (up to 40% by volume). At the higher concentrations the particle interactions are taken into consideration by the supported load σ_{SL} (i.e., coulombic contacts), dispersive stress σ_{DS} (i.e., particle collisions), and increased diffusivity ϵ_S (i.e., mixing effects).

The differential equations for solid velocity and concentration distributions in a horizontal pipe cross section are

$$\left(\frac{\partial^2}{\partial x^2}+\frac{\partial^2}{\partial y^2}\right)\left((\mu_M-\mu_L)V_M+C\rho_S\alpha_S V_S^2\right)-C\frac{dp}{dz}-\text{sign}\left(\frac{\partial V_S}{\partial y}\right)\cdot\frac{\partial}{\partial y}(\sigma_{SL}\tan\beta)+(R_{Sz})_L=0 \quad (1)$$

$$\frac{\epsilon_s{}^2}{W^2}\cdot\left|\text{grad } C\right|\cdot\text{grad } C+\frac{\rho_S C}{(\rho_S-\rho_L)g}\cdot\text{grad }\sigma_S+C^2\bar{e}_y=0 \quad (2)$$

where

x,y,x	= horizontal, vertical, and axial direction, respectively
V_M,V_S	= mixture and solid velocity in the axial direction, respectively, m/s
ρ_L,ρ_S	= density of liquid and solid phase, respectively, kg/m^3
μ_L,μ_M	= liquid and mixture dynamic viscosity, respectively, Ns/m^2
C	= solid concentration (by volume)
p	= pressure, N/m^2
α_S	= turbulence index for solid phase, m
ϵ_S	= diffusion coefficient of solid particles, m^2/s
τ_S	= shear stress between solid particles, N/m^2
σ_{SL}	= normal stress between solid particles in coulombic contact, N/m^2
σ_S	$=\frac{\tau_S}{\tan\theta}+\sigma_{SL}\left(1-\frac{\tan\beta}{\tan\theta}\right)$, normal stress between solid particles, N/m^2
$\tan\beta,\tan\theta$	= coefficients of sliding and dynamic friction between solid particles, respectively
$(R_{Sz})_L$	$=C\frac{3}{4}\frac{\rho_L C_{DS}}{d}\frac{\lvert V_M-V_S\rvert(V_M-V_S)}{(1-C)^{3.7}}-(1-C)dp/dz$, interaction term
W	= hindered settling velocity, m/s
C_{DS}	= hindered drag coefficient
$\bar{e}_y$	= vertical unit vector

Equation 1 is the momentum equation for the solid phase in the axial direction and is solved after the mixture velocity is detemined

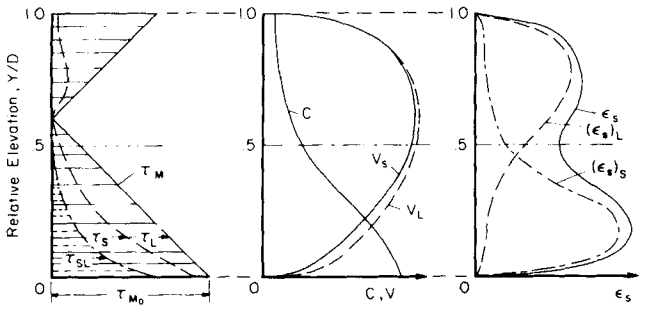

Figure 1. Scheme for flow parameter distributions.

(Roco and Shook, 1983a). The coefficients $\tan\beta$ and $\tan\theta$ take values about 0.3 and 0.5, respectively. The interaction term between phases in the axial direction $(R_{Sz})_L$ has a drag component, which is a function of the velocity difference $(V_M - V_S)$, and a pressure component due to the total headloss along the pipe.

Other terms were discussed in previous papers (Roco and Shook, 1983a,b); the calculation of the diffusion coefficient ϵ_S is explained below. An equivalent distance for the diffusion process in the carrier liquid alone is used for this purpose. To adjust the calculation for the presence of solid particles in the mixture flow, the distance y from the wall is replaced by the equivalent distance y_ϵ. The condition that the same increase of ϵ_S occurs along δy_ϵ in mixture (concentration C) as would occur along δy at $C = 0$ for the same diffusion flux gives

$$\frac{\delta y_\epsilon}{\delta y} = \frac{\delta \epsilon_L(y)}{\delta \epsilon_S(y)} = \phi_S(C, Fr_*) \tag{3}$$

where ϕ_S is a coefficient dependent on the local concentration (C) and turbulence intensity expressed by a modified Froude number Fr_* (Roco and Shook, 1983b). The value of ϵ_S at a position y from the wall is then computed from y_ϵ:

$$y_\epsilon = \sum_{1,N} \delta y_{\epsilon i} = \sum_{1,N} \delta y_i \cdot \phi_{Si} \tag{4}$$

where $\delta y_{\epsilon i}$ is the equivalent length in the pure fluid corresponding to the geometrical length δy_i.

An alternative to determine ϵ_S (by solving a transport equation) was previously presented (Roco and Balakrishnan, 1982).

Typical variations of the main flow parameters in the vertical midplane are shown in Figure 1. One observes that the total mixture shear stress (τ_M) has a component due to liquid (τ_L) and another due to the solid phase (τ_S). A part of τ_S is used to overcome the coulombic friction (τ_{SL}), and the difference ($\tau_S - \tau_{SL}$) is used to maintain the flow shear rate. The solid velocity distribution at the bottom V_S is expected to have a specific shape for a sliding or a fixed bed of particles. The solid concentration (C) has a determinant influence on the relative velocity between liquid and solids $(V_L - V_S)$, as well as on the contribution of liquid $\epsilon_{S(L)}$ and solid $\epsilon_{S(S)}$ phases in the total diffusion coefficient ϵ_S.

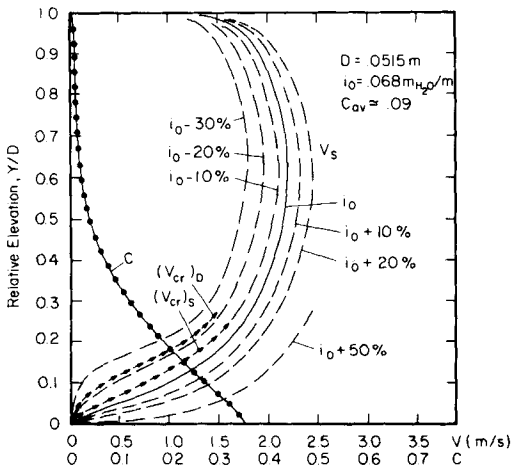

Figure 2. Solid velocity (V_S) and concentration (C) distributions in 51.5 mm pipe: run A1.

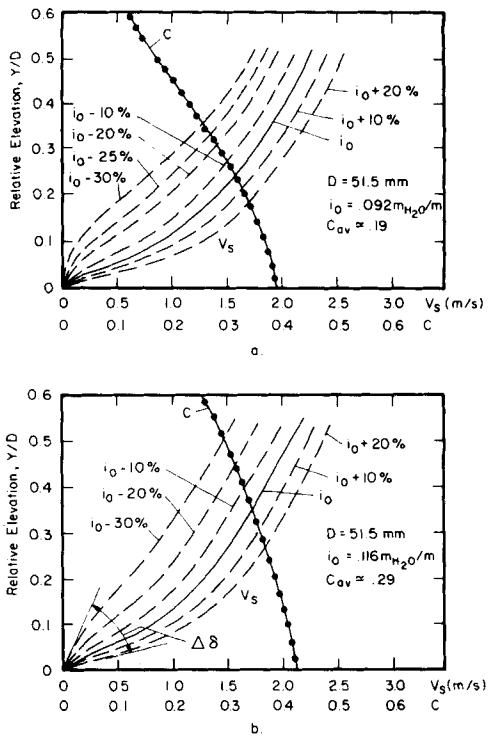

Figure 3. Solid velocity (V_S) and concentration (C) distributions in 51.5 mm pipe: *a*, run A3; *b*, run A5.

Equation 1 provides the solid velocity distribution for laminar and turbulent flow of uniform particles in horizontal pipes. It can be extended to multispecies particle flow (Roco and Shook, 1984) and other flow conditions (inclined pipes and channels, various rheological characteristics) by remodeling some constitutive terms. The critical flow regime can be interpreted in all these situations based on the shape of the V_S curve at the lower boundary.

RESULTS AND DISCUSSION

The model application is illustrated with results on flowing water-sand mixtures in pipes.

The sand particles are of a quasiuniform size about $d_{50\%} = 0.165$ mm, with rounded edges. The measurements of mean velocity and concentration distributions were made with a precision of 3% (Roco and Shook, 1983b) and were verified by integral measurements in the cross section with a magnetic flowmeter and by volumetric means. The critical sediment velocity was estimated by visual observation at transparent pipe sections and by using a heated sensor proposed by Ercolani et al. (1979). The formation of a sliding layer of solid particles on the pipe bottom was visually observed for the threshold velocity.

We focus our attention on the shape of the solid particle velocity distribution in the bottom region.

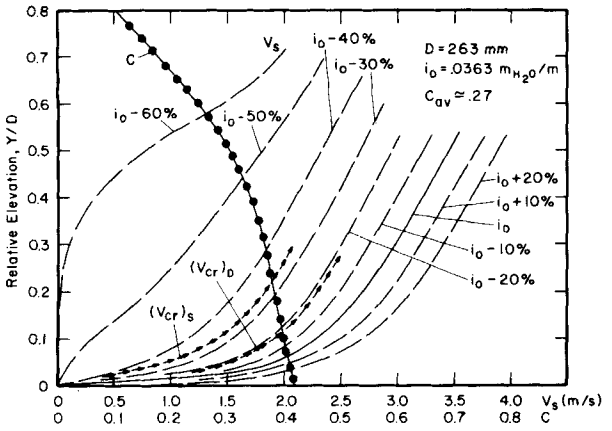

(a)

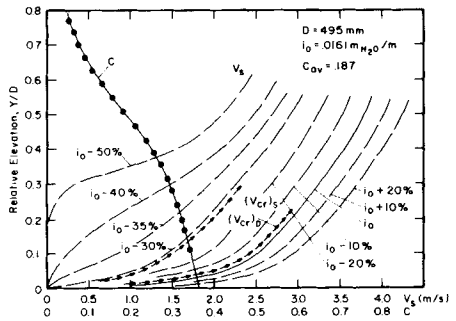

(b)

Figure 4. Solid velocity (V_S) and concentration (C) distributions in 263 and 495 mm pipes: *a*, run A11; *b*, run A17.

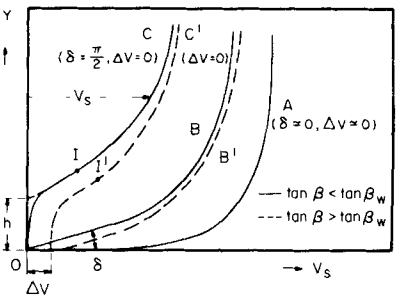

Figure 5. Scheme for velocity distribution (V_S) at lower boundary: *A*, only suspension; *B,B'*, with sheared bed of particles; *C,C'*, with compact bed of particles (C = stationary bed, C' = sliding bed).

Let us consider variations of the headlosses between −30% and +50% about a flow situation ($i = i_o$), for which the computed distributions of the solid velocity and concentration were experimentally verified (Figure 2, test A1). The visual observations in the laboratory indicated a regime close to the critical velocity. We assume in computation the experimental concentration distribution as given, equal to the experimental data measured at i_o. The velocity profiles change with the headlosses especially at the pipe bottom. While for higher headlosses ($i = i_o + 50\%$) the velocity curve is practically tangent to the horizontal lower boundary, at smaller headlosses the curve detaches from the bottom under an increasing angle (δ). Concurrent with the reduction of the average velocity in the cross section, the shape of the lower velocity curve changes. From a quasilinear profile ($i = i_o$ to $i_o + 50\%$) at the pipe bottom, the curve begins to have an inflection point ($i = i_o - 10\%$ to $i_o - 30\%$), and for $i = i_o - 30\%$ is tangent at the origin to the vertical axis.

Let us consider two empirical correlations for critical deposit velocity proposed by Durand (1953) and Silin (1971), each tested on a large set of experimental data. The Durand formula gives $(V_{cr})_D = 0.87$ m/s, while the Silin formula predicts $(V_{cr})_S = 1.17$ m/s. The first result would correspond to $i_o - 22\%$ and the second to $i_o - 10\%$. It appears that the two predictions would correspond to two different moments (two angles δ) in the transition between sliding and stationary bed of particles.

Figure 3 shows velocity profiles in the bottom region with concentrations higher than that employed in run A1. One observes that the domain of variation of the angle δ, $\Delta\delta$, diminishes for the same percentage variation of the headlosses (for instance, between i_o − 30% and i_o + 20%). The same tendency was observed when the pipe diameter is larger (Figure 4). Both situations may be justified by the increased mixing effects at higher concentrations and larger pipe diameters.

In our tests with 0.165 mm sand it was assumed that the friction coefficient between solid particles and pipe wall ($\tan\beta_W$) exceeds the coefficient of dynamic friction between particles ($\tan\beta = 0.3$). This would correspond to the solid lines in Figure 5, where flows without deposition (A), with a sheared bed (B), and with stationary compact bed (C) of particles are suggested. When $\tan\beta_W < \tan\beta$, both sheared and coulombic contact layers of particles have a relative velocity (ΔV) compared to the wall (dashed lines in Figure 5, B' and C'). When the shear rate in the "bed" of particles is smaller than the shear rate in the mixture in the immediate vicinity of the bed, the inflection point occurs (I and I' in Figure 5). The critical velocity may be defined as the averaged velocity in pipe for which (a) the angle δ takes a chosen value (over 5–10°), or (b) the inflection point occurs, or (c) the compact bed of particles begins to develop ($\delta \simeq 90°$). The first layer of particles in contact with the wall may be stationary ($\Delta V \approx 0$) or sliding ($\Delta V \approx 0$). The moment of aparition of the inflection point best defines the unstable critical flow regime, in which the specific fluctuating velocities develop.

Direct visual observations confirm the turbulent stochastic character of the flow. In the transition zone $0° < \delta < 90°$, concentration and velocity fluctuations of low frequency are observed whose time average values represent the predictions made here.

CONCLUSIONS

A criterion for the critical velocity is suggested based on the velocity distribution of solid particles in the vicinity of the pipe bottom. The inflection point characterizes the critical flow regime. It depends on the flow structure in the flow cross section and may be applied for dilute and dense slurry flows ($C < 40\%$). The approach can be used as a framework to interpret experimental results.

The numerical method for critical velocity provides a way to generalize and scale-up experimental results on critical flow rate in slurry flows. It can be extended to other flow situations (multispecies particle flow, inclined pipes and channels, centrifuges) for which previous empiricial approaches are insufficient.

ACKNOWLEDGMENT

The studies reported here were supported by NSF Grant CPE 8205217 and Canadian NSERC A1037.

NOTATION

C = solid concentration, by volume
C_{DS} = hindered drag coefficient
$d_{50\%}$ = 50% (mass) solid particle diameter
D = pipe diameter
$\bar{e}_y$ = vertical unit vector in the y direction
$Fr*$ = $\rho_L/\rho_M \cdot V_*^2/gd(s-1)$ = modified Froude number of particles, where $V*$ is the friction velocity
$F(d_{50\%},C)$ = experimental function
g = gravitational acceleration
h = height of the compact bed of particles
i = hydraulic gradient, m of water/m of pipe
i_o = reference hydraulic gradient
N = number of segments δ_{yi}, defined in Eq. 4
p = pressure
$(R_{Sz})_L$ = interaction term, of liquid on solid phase in the z direction
S = density ratio of solids to fluid
V = velocity in the axial direction
$(V_{cr})_D$ = $F(d_{50\%},C) \cdot [2gD(\rho_S/\rho_L - 1)]^{.05}$, critical velocity after Durand (1953)
$(V_{cr})_S$ = $8.22 \cdot D^{.33} \cdot C^{.167} [W^2/(2gD(\rho_S - \rho_L))]^{.0625}$, critical velocity after Silin (1971)
W = hindered settling velocity
x,y,z = horizontal, vertical, and axial coordinates, respectively

Greek Letters

ϵ = diffusion coefficient
α = turbulence index
$\tan\beta,\tan\theta$ = coefficients of sliding and dynamic friction between solid particles, respectively
μ = dynamic viscosity
ρ = density
τ = stress
σ = normal stress
δ = angle between the curve V_S and wall at $y = 0$
ϕ_S = coefficient for the influence of solid particles on diffusion
ΔV = sliding velocity of solids at the pipe wall

Subscripts

av = average
L = liquid
S = solid
M = mixture
SL = due to supported load, transmitted by coulombic contact between solid particles
ϵ = used for ϵ calculation
$(\ldots)_L$ = due to liquid
$(\ldots)_S$ = due to solid

LITERATURE CITED

Bain, A. G., and S. I. Bonnington, *The Hydraulic Transport of Solids by Pipelines*, 19, Pergamon, New York (1970).

Durand, R., "Basic Relationships of the Transportation of Solids in Pipes—Experimental Research," *Proc. Int. Assoc. Hydraulic Res.*, Minneapolis (1953).

Ercolani, D., F. Ferrini, and V. Arrigoni, "Electric and Thermic Probes for Measuring the Limit Deposity Velocity," Hydrotransport 6 Conf., Paper A2, 13 (1979).

Hanks, K. W., and D. G. Sloan, "A Rheology-based Correlation for Minimum Deposition Velocities," *Proc. 6th Slurry Transport Assoc. Conf.*, **6**, 107 (1981).

Raudkivi, A. J., *Loose Boundary Hydraulics*, Pergamon, New York (1976).

Roco, M. C., and N. Balakrishnan, "Multidimensional Flow Analysis of Solid-Liquid Mixtures," Proc. 54th Ann. Meeting of the Soc. of Rheology (1982), (also *J. of Rheology*, **29**, No. 4, 1985).

Roco, M. C., and C. A. Shook, "Modeling Slurry Flow: The Effect of Particle Size," *Can. J. Chem. Eng.*, **61**, 494 (1983a).

——, "Turbulent Flow of Incompressible Mixtures," *4th Symp. Turbulent Shear Flow*, Karlsruhe, 12.1 (1983b), (also *J. of Fluids Eng.*, **107**, 1985).

——, "Computational Method for Coal Slurry Pipelines with Heterogeneous Size Distribution," *J. Powder Technol.*, **38** (1984).

Silin, N. A., et al., *Hydrotransport* (In Russian), Ed. Nauka, Kiev (1971).

Wiedenroth, W., and H. Kirchner, "Critical Velocity Calculation and Slurry Pipelines Optimization," *Hydrotransport 2 Conference*, BHRA, Paper E1, England (1972).

Manuscript received Dec. 7, 1983; revision received June 26 and accepted July 3, 1984.